Effect of Simulated Jet Engines on the Flowfield behind a Swept-Back Wing

Z. El-Ramly* and W. J. Rainbird†
Carleton University, Ottawa, Canada

Measurements of the vortex behind a swept-back wing have been made in a low-speed wind tunnel. Results have been taken with a clean wing, with engines mounted in representative positions, and with and without jet exhaust simulation. Only cruising flight conditions are simulated. Loading on the wing has been obtained from pressure distribution measurements. Flowfield properties and the rolling moment on a trailing wing have been measured at 2½ and 5 wing spans downstream. The concentrated tip vortex structure is essentially unaffected by the engines but the remaining shear layers are considerably distorted by the pylon-nacelles. The maximum induced rolling moment on the trailing wing is only slightly reduced by the present engine installation or the simulated jet exhaust.

Introduction

DURING flight tests conducted by the Federal Aviation Administration (FAA) (see Ref. 1) a distinct characteristic peculiar to T-tail aircraft with engines mounted on the rear fuselage was observed, namely that these aircraft produce more persistent trailing vortices with much higher tangential velocities than aircraft with engines mounted under the wing. This difference might be attributed to one of the following three factors or a combination thereof: 1) the T-tail (an unlikely contributor), 2) the lack of high-velocity engine exhaust jets injecting directly into the developing vortex flowfield, or 3) the lack of engine pylons and nacelles on the underside of the wing, thereby producing a "clean" wing configuration with uninterrupted boundary-layer development and outboard flow of the resulting free shear layers (which form the vortex wake).

There do not appear to be many systematic wind tunnel measurements to investigate these differences in vortex development due to aircraft configuration. Chigier and Corsiglia in Ref. 2 have reported on some hot-wire measurements behind a semispan model of a CV-990 aircraft. Their wind tunnel model has open engine-nacelles (without high total pressure jet exhaust simulation), antishock bodies, and flaps; however, it is not possible from their results to identify the separate effects of these different components on the flowfield. Wickens in Ref. 3 has made wind tunnel measurements of the flowfield behind a quasi-two-dimensional wing, with a simulated high bypass ratio engine and externally blown flap configuration. However, these and other similar measurements have been primarily designed to elucidate the local aerodynamic details of the externally blown flap as a high-lift device rather than to study vortex roll-up and complete wake structure.

Recently the Boeing B-747 aircraft has been the subject of several flight, wind tunnel, and tow tank tests.[4-9] The models used have most of the details of the B-747; moreover, almost all of these measurements were made to investigate the landing case with large flap deflections, resulting in multiple vortices and adding to the complexity of the flowfield. Again it is not possible to separate the effects of engine installation in these measurements, especially since only flow visualization and/or induced rolling moment measurements were made. Some of these measurements,[6-8] however, examined the effect of thrust by comparing the induced rolling moment for idle and level flight thrust. For some particular landing flap configurations, the effect of thrust appears to be significant; however, because of the multiple vortex structure it is not possible to define the mechanism by which the jet thrust (engine exhaust) affects the vortex system.

In addition there have been a number of studies of the effect on core structure and decay of directly blowing a jet along the vortex axis (Ref. 10 is a recent example, and Refs. 11 and 12 include a survey of relevant measurements). While such experiments approximately simulate a wingtip-mounted engine installation, they do not explain how the engine exhaust ultimately mixes with the trailing vortex system for conventional wing-mounted engines. Thus there is a need for further experimental studies to clarify the role of wing-mounted engine installations on trailing vortex structure. If a model wing can be built that has removable pylons and nacelles, and simulated jet exhausts, then it should be possible to study the vortex system without the simulated engines mounted, that is in the "clean" wing configuration, then, by adding the engines, study the resulting interference effects on the flowfield. The present paper describes a limited attempt at such an investigation for conditions representative of cruising flight.

Experimental Set-Up

The present experiments have been carried out in the 20×30-in. low-speed closed return circuit wind tunnel at Carleton University. The flow in the 22-ft-long working section, following the 12:1 contraction, is of good quality with mean flow angularity within ±0.15 deg, streamwise component of turbulence approximately 0.1% and essentially zero axial gradient of static pressure. Figure 1 shows a schematic layout of the working section. A more complete description of the test apparatus can be found in Refs. 12 and 13, but the characteristics of the main and intercepting wing are repeated here, in Table 1, for completeness.

The simulated jet engines, Fig. 2, were designed to represent a Boeing 747 with JT9D engines. While the physical scale and position have been approximately represented, the detailed geometry of the pylon and nacelle are not, of course, correct; also the inlet has been faired in. The jets are supplied with unheated high-pressure air (from a 100 psi lab source) through separate 3/8-in. copper tubes embedded in the half-

Presented as Paper 76-63 at the AIAA 14th Aerospace Sciences Meeting, Washington, D.C., Jan. 26-28, 1976; submitted Feb. 3, 1976; revision received Nov. 11, 1976.

Index categories: Aircraft Aerodynamics (including Component Aerodynamics); Aircraft Testing (including Component Wind Tunnel Testing); Jets, Wakes, and Viscid-Inviscid Flow Interactions.

*Research Associate, Dept. of Mechanical and Aeronautical Engineering. Member AIAA.

†Professor of Engineering, Dept. of Mechanical and Aeronautical Engineering. Member AIAA.

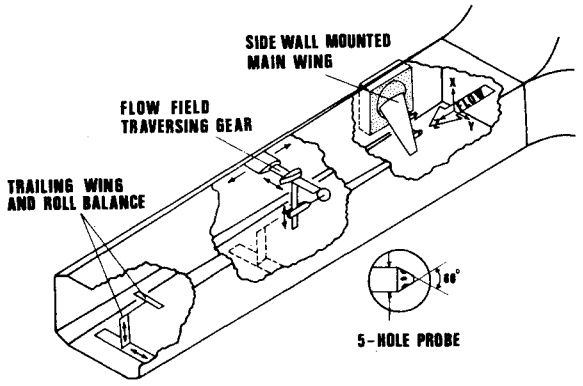

Fig. 1 Isometric sketch of working section.

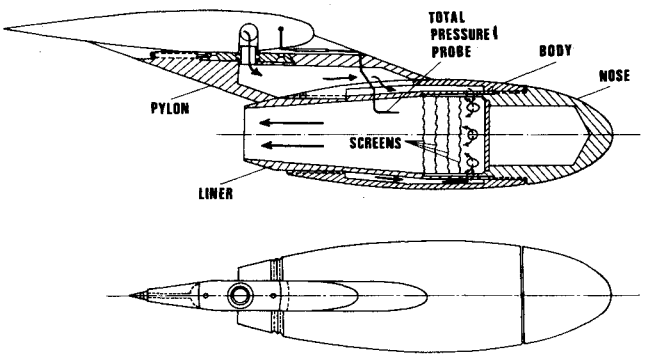

Fig. 2 Simulated jet engine.

wing. Each supply pipe has four outlets corresponding to alternative spanwise mounting positions for each engine. For the present experiments the inboard engine was attached at a spanwise position $2y/b = 0.40$ and the outboard engine was at 0.67, closely simulating the layout of the B-747.

It is clearly not possible to easily simulate the mixed flow exhaust of the JT9D engines with the varying exit velocities and densities in the two streams. Instead we have used jets of the correct overall relative scale and have attempted to get the external mixing approximately correct by using a jet exit velocity to freestream velocity ratio of 1.5. This ratio is representative of cruising flight conditions and is compatible with the relatively low wing lift coefficients available with the present small scale installation. Details of the design, sizing, and calibration of the simulated engines can be found in Ref. 12. The exit plane jet dynamic pressure nonuniformities have been reduced to better than ±4% by using three 0.25 open-area-ratio screens followed by one 0.54 open-area-ratio screen and a 2.3:1 conical contraction downstream of the throttling ring (see Fig. 2). The jet exit plane conditions for each engine have been calibrated using an internal total pressure probe and the measured variation of exhaust static pressure with wing angle of attack.

Due to the inadequate volume flow capacity of the shop air supply used to feed the engines it was not possible to maintain the required jet velocity ratio of 1.5 above a working section speed of about 115 fps ($R_c = 0.34 \times 10^6$) well below the maximum working section speed of 175 fps ($R_c = 0.50 \times 10^6$).

Measurements of the flowfield, using a calibrated non-nulling blunted conical 5-hole probe, as well as induced rolling moments on an intercepting wing (Table 1) were made at two positions 2½ and 5 wing spans downstream. The probe was calibrated at angles up to the cone half-angle of 30 deg; details of the probe calibration and the accuracy of the resulting flowfield measurements can be found in Refs. 12 and 14. The effect of the engine pylon and nacelle combination (with and without air injection) on the chordwise and spanwise loading was also obtained by pressure plotting at appropriate spanwise positions on the main wing. Results will be presented for two angles of attack $\alpha = 5$ deg, corresponding to $C_L = 0.34$ for the clean wing configuraion and representative of cruise conditions; and $\alpha = 11$ deg, $C_L = 0.74$, which is the maximum angle of attack attainable before extensive leading-edge separation occurs near the wingtip.

Table 1 Wing dimensions[a]

	Main (half) wing	Trailing wing
Span	21.0 in. (×2)	10.0 in.
Relative span	1	0.24
Average chord	6.00 in.	1.33 in.
Aspect ratio	7.0	7.5
Taper ratio	1/3	1
Sweepback (¼c)	35 deg	0 deg
Wing twist	0 deg	0 deg
Wing section	12%, symmetrical	NACA 64_2-015
Tip form	half body	square cut

[a]Transition fixing on trailing wing with sand roughness strip (0.0057-0.0072 in.) to 15% chord on both surfaces.

Discussion of Results

The lifting characteristics of the generating half-wing (herein called main wing) in the clean configuration, and of the trailing wing, have been reported in Refs. 12 and 13. The effect of engine pylon and nacelle on the main wing loading is shown in Fig. 3. For $\alpha = 11$ deg, $C_L = 0.74$, the effects are local and more or less confined to spanwise stations near the pylons, although there is some tendency for higher loading near the tip with engines mounted. The change in the overall lift coefficient is nevertheless negligible. For $\alpha = 5$ deg, however, engine pylon and nacelle effects on the main wing loading are more than local. There is a general decrease in local lift coefficient, outboard of the inboard engine, resulting in a reduction of overall lift coefficient of about 5%. No appreciable additional effect of air injection (simulating the jet exhaust) on the main wing loading was noticed.

Before starting the discussion of the flowfield results, it might be helpful to briefly clarify the relation between the viscous wake and the so-called trailing vorticity. In the usual idealized inviscid flow analysis the flow immediately behind an isolated wing with the Kutta condition applied consists of a nearly plane vortex sheet (wake) stretching across the span of the wing. Within a short distance downstream, the vortex sheet curls up at the free edges and forms a pair of nearly axisymmetric trailing vortices, concentrating a large portion of the vorticity from the vortex sheet into the cores of the vortex pair. By contrast in the real viscous case, the boundary layers on the upper and lower surfaces of the wing, with their

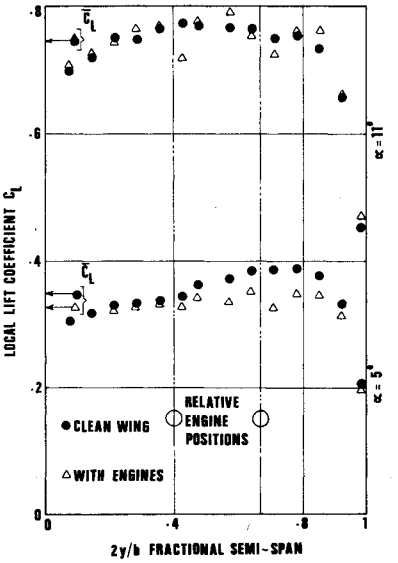

Fig. 3 Effect of engines on spanwise loading.

vorticity (including that associated with lift), form a free shear layer of finite but small thickness which leaves the wing from the separation lines and trails behind the wing as the viscous wake. The flow near the wingtip is of course highly three-dimensional and the vorticity vectors there are far from being in the streamwise direction. The Helmholz theorem requires that the vorticity adhere to the fluid particles; consequently the vorticity must remain in the free shear layer and thus we should expect (even with diffusion) to find the shed vorticity contained within the viscous wake at any downstream position. Detailed flowfield surveys behind swept-back wings by DeVries[15,16] and by the present authors[17,18] have confirmed that the vorticity is contained within the viscous wake with the "center" of the trailing vorticity located somewhat above the center (minimum total pressure) of the viscous wake.

The effect of the engines on the wake, with and without the exhaust flow simulation ($V_j/V_\infty = 1.5$), is best demonstrated by Figs. 4 and 5, which show the contours of equal total pressure loss coefficient for $\alpha = 5$ and 11 deg at the 2½b station for the flowfield outboard of mid-semispan. As previously discussed, the viscous wake contains all the shed vorticity and its development traces and defines the vortical wake. The rolled-up part of the shear layer, "the core," does not seem to have been appreciably changed; however, the still unrolled part has been considerably distorted and its spiralling "roll-up" into the inner core interrupted. This wavy deformation of the unrolled-up shear layer is consistent with, and might be due to, significant side forces on the pylon-nacelles which are not canted outwards in the experiment but attached to the wing in a direction parallel to the root chord. Careful examination of Figs. 4 and 5 will also show that this shear layer deformation and interruption of the roll-up is just the result of mounting the engines, i.e., a pylon-nacelle effect, and is not due to the air injection as such. The dominant effect of air injection on the total pressure loss is to remove the high-loss region marking the wake of the engine nacelles (with blowing). The shear layer originating from the main wing and pylons is approximately the same shape with and without injection. Another interesting feature of the flow is that the jet exhaust from each engine, while considerably enlarged and

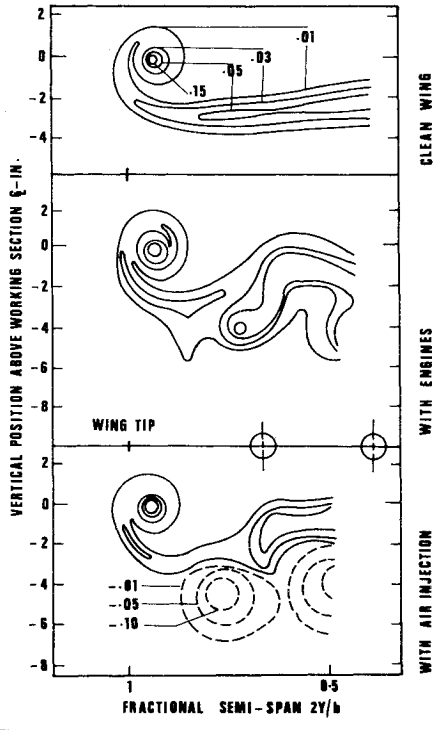

Fig. 4 Contours of equal total pressure loss coefficient ($P_{0\infty} - P_0)/½\rho V_\infty^2$, ($\alpha = 5$ deg, 2½b).

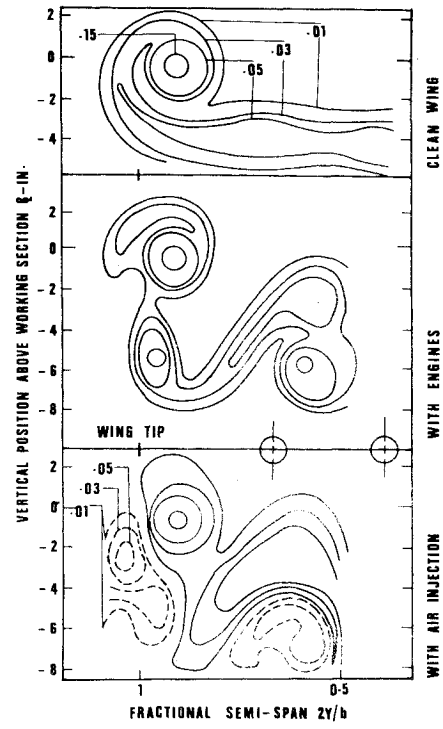

Fig. 5 Contours of equal total pressure loss coefficient ($P_{0\infty} - P_0)/½\rho V_\infty^2$, ($\alpha = 11$ deg, 2½b).

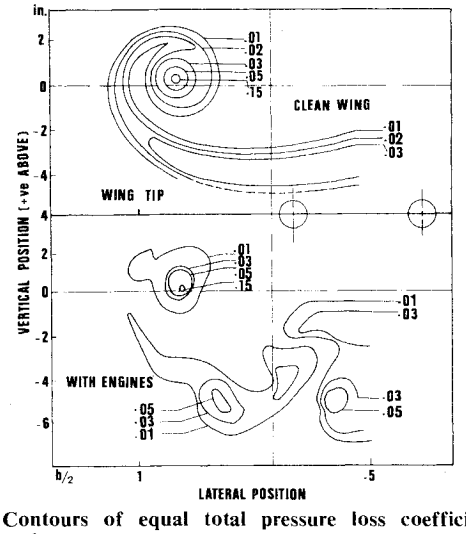

Fig. 6 Contours of equal total pressure loss coefficient ($P_{0\infty} - P_0/½\rho V_\infty^2$, ($\alpha = 5$ deg, 5b).

distorted as a result of mixing with the surrounding airflow, still appears as separate and distinct total pressure rise contours (shown dotted on the lower parts of Figs. 4 and 5). Because of the relatively higher induced cross-flow velocities for $\alpha = 11$ deg, $C_L = 0.74$, than for $\alpha = 5$ deg, $C_L = 0.34$, the high pressure exhaust from both engines (or the region of high total pressure loss marking the nacelle wake for the no injection case) has obviously "drifted" more outboard for $\alpha = 11$ deg than for $\alpha = 5$ deg.

Figure 6 gives the results of the limited total pressure loss measurements made at the 5b station with the clean wing configuration and with engines mounted but no air injection, at $\alpha = 5$ deg. The orderly flow with the shear layer spiralling into the core for the clean wing case is disrupted by the mounting of the engines, resulting in a relatively isolated core and a break up of the remnant shear layer (and the associated vorticity shed from that region of the wing from which this part of the shear layer originated).

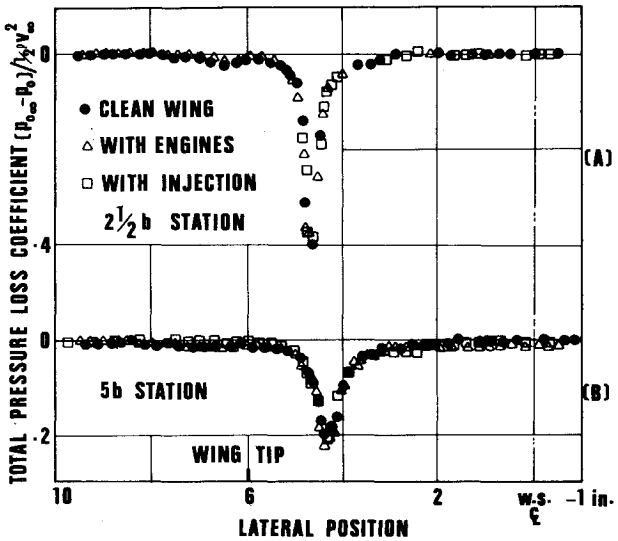

Fig. 7 Total pressure loss coefficient, $\alpha = 5$ deg: lateral scans through vortex center.

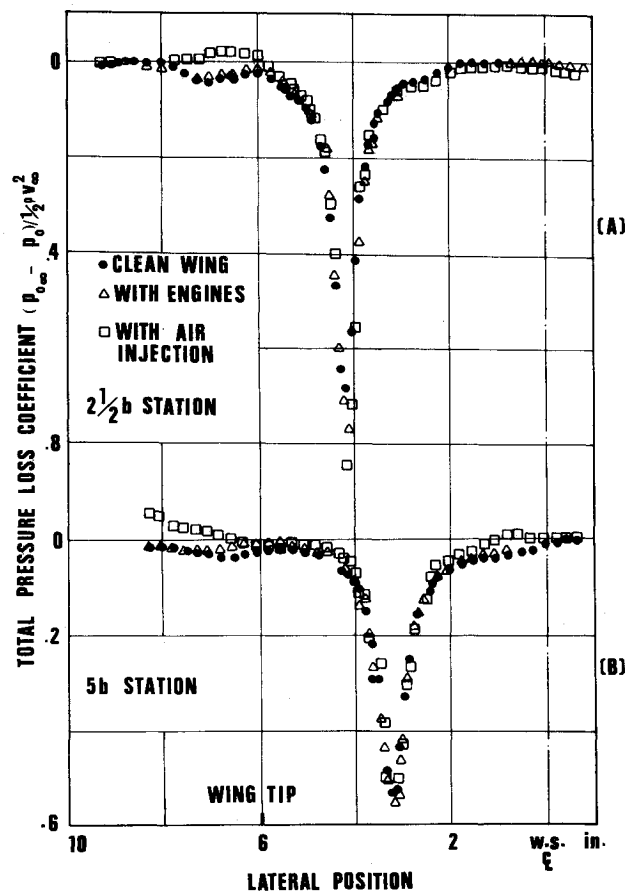

Fig. 8 Total pressure loss coefficient, $\alpha = 11$ deg: lateral scans through vortex center.

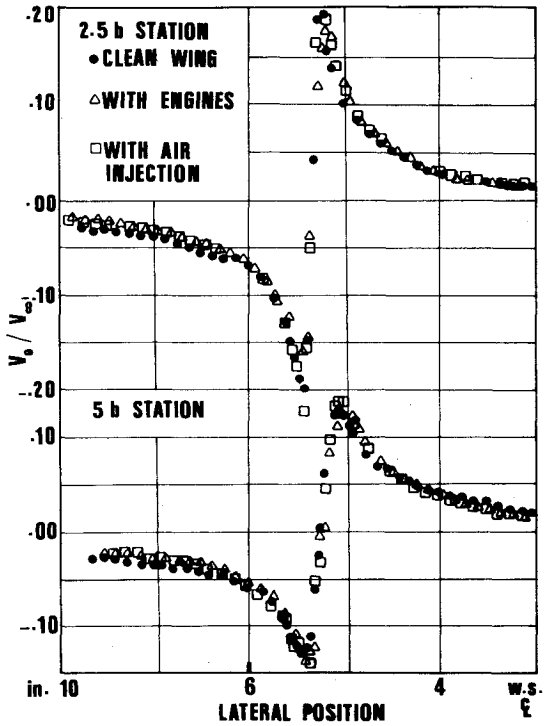

Fig. 9 Tangential velocity profile, $\alpha = 5$ deg.

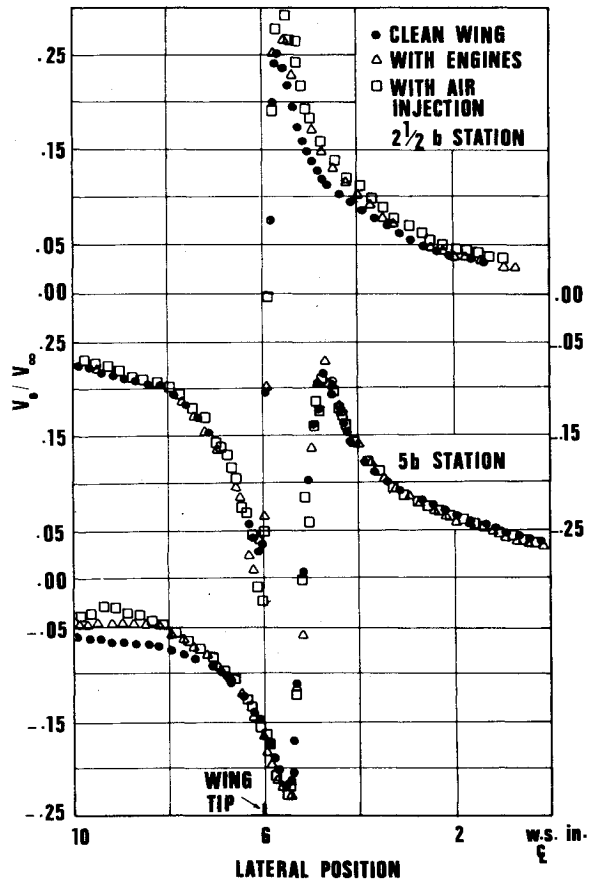

Fig. 10 Tangential velocity profile, $\alpha = 11$ deg.

Figures 7 to 10 show quantitative flowfield results obtained with the 5-hole probe when scanned laterally through the vortex center. Figures 7 and 8 show the variation of the total pressure loss coefficient for $\alpha = 5$ and 11 deg, respectively. As concluded from Figs. 4 and 5, the concentrated vortex core does not seem to have changed appreciably even though the spiralling "roll-up" of the shear layer into it has been interrupted. Clearly the size and shape of the regions of high total pressure loss are very similar for all configurations. Some apparent variation of the maximum total pressure loss could have resulted from missing the vortex center by even a very small distance because of the steep gradient there. The position of the vortex center was found to vary slightly for the different configurations tested (see also Figs. 4-6) and some of the profiles presented in Figs. 7-10 were shifted (maximum of 1/4 in.) to match the vortex centers and facilitate comparison.

Figure 8b shows, for $\alpha = 11$ deg, a region of total pressure excess far outboard of the core at the 5b station with air in-

jection. This region marks the jet exhaust of the outboard engine, still spiralling (rolling up) around the core and as yet not completely mixed with it. Without air injection the bump in the total pressure loss coefficient is further outboard of the core with engines mounted as compared to the clean wing configuration, indicating an interruption to the roll-up.

The tangential velocity profiles (Figs. 9 and 10 for $\alpha = 5$ and 11 deg, respectively) quantitatively reflect the effects of the changes in spanwise loading and in the nature of the roll-up. For $\alpha = 5$ deg, Fig. 9 shows that with engines mounted, but no air injection, there is a general decrease in the induced tangential velocities which is at least partly due to the decrease in the overall lift coefficient. The decrease in the tangential velocity level is more evident at the 5b station simply because the rolled up part is more symmetrical than at the 2½b station (see also the total pressure loss contours on Figs. 4 and 6). However, for $\alpha = 11$ deg, at the 2½b station, Fig. 10a shows that the induced tangential velocities with engines mounted are somewhat higher than for the clean wing configuration, particularly inboard of the core. This could be a result of the slightly higher loading near the tip with engines mounted (see Fig. 3). Figure 5 shows that the core is more symmetrical for this case with engines mounted and this is also reflected in the corresponding tangential velocity profile. As discussed before, the addition of air injection has a negligible effect on the wing loading and Figs. 9 and 10 confirm that it has a correspondingly negligible effect on the induced tangential velocities.

Probably the best and most convenient way to assess the effects of engines on the flowfield from the hazard-to-following-aircraft point of view is to measure the induced rolling moment on a representative trailing wing. Figures 11 and 12 and Table 2 show the results of such measurements. Figure 11 gives the variation of the induced rolling moment coefficient on the trailing wing when it is scanned vertically with its axis (sting mount) in the same lateral plane as the vortex center generated by the main wing with engines mounted but with no air injection. Also shown in Fig. 11 is the level of the maximum induced rolling moment coefficient for the clean wing configuration which, according to Ref. 13, does not change between the 2½ and 5b stations. The curves representing data at the 5b station have been traced directly from the x-y plotter output, without averaging, to show local perturbations.

For $\alpha = 5$ deg the maximum induced rolling moment coefficient is about 12% lower than for the clean wing configuration (see Table 2) at both the 2½ and 5b stations, in agreement with the lower induced tangential velocities. Mounting the engines has resulted in a decrease of overall lift coefficient of about 5%, consequently the decrease in the induced rolling moment coefficient normalized to the generating wing overall lift coefficient C_{ℓ}/C_L (which is the actual measure of hazard) is only about 7%. References 12 and 13 have shown that for the clean wing configuration (for the same experimental set-up) only about 42% of the circulation derived from the spanwise loading was concentrated in a rolled up core and the fraction that rolled up was that shed from near the wingtip. Consequently, it is to be expected that the 5% decrease in overall $\bar{C}_L$ with engines mounted will result in an even larger percentage decrease in the circulation around the rolled up part as is indicated by the measured maximum induced rolling moment.

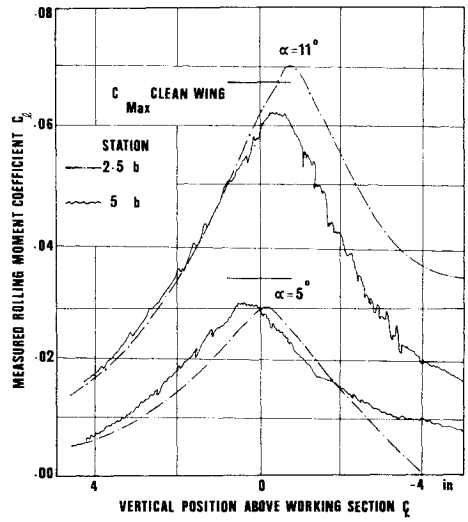

Fig. 11 Induced rolling moment on trailing wing with engines mounted.

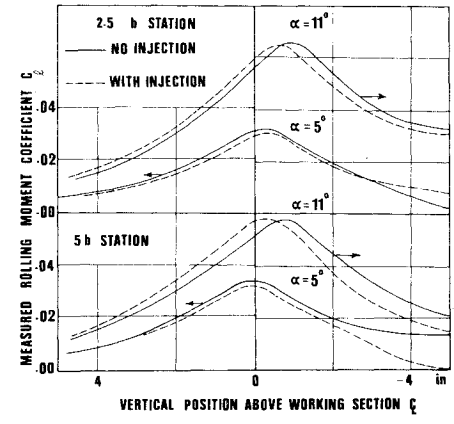

Fig. 12 Induced rolling moment coefficient on trailing wing: effect of simulated jet.

Table 2 Maximum induced rolling moment coefficient on trailing wing

	Clean wing ($R_{\ell} = 0.5 \times 10^6$)		With engines ($R_{\ell} = 0.5 \times 10^6$)		With engines ($R_{\ell} = 0.34 \times 10^6$)		With air injection ($R_{\ell} = 0.34 \times 10^6$)	
	C_{ℓ}	$C_{\ell}/\bar{C}_L$	C_{ℓ}	$C_{\ell}/\bar{C}_L$	C_{ℓ}	$C_{\ell}/\bar{C}_L$	C_{ℓ}	$C_{\ell}/\bar{C}_L$
2½ b station								
$\alpha = 5$ deg								
measured	0.034	0.100	0.030	0.092	0.030	0.092	0.031	0.095
calculated	0.039	0.114			0.033	0.010	0.034	0.105
$\alpha = 11$ deg								
measured	0.067	0.091	0.069	0.093	0.065	0.088	0.066	0.087
calculated	0.074	0.101			0.074	0.101	0.075	
5 b station								
$\alpha = 5$ deg								
measured	0.036	0.105	0.031	0.095	0.032	0.098	0.033	0.101
calculated	0.038	0.111	0.032	0.098	0.034	0.105	0.034	0.105
$\alpha = 11$ deg								
measured	0.067	0.091	0.062	0.084	0.058	0.078	0.057	0.077
calculated	0.078	0.106	0.067	0.091	0.067	0.091	0.063	0.086

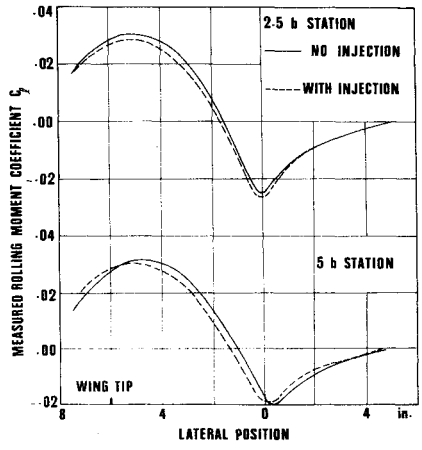

Fig. 13 Induced rolling moment coefficient on trailing wing: variation with lateral position.

For $\alpha = 11$ deg, at the 2½b station, the maximum induced rolling moment with engines mounted is slightly higher than for the clean wing configuration (upper curve on Fig. 11). Again this is in agreement with the measured tangential velocities, and might be the result of the higher loading near the main wingtip, as discussed above ($\bar{C}_L$ did not change with engine mounting – see Fig. 3).

For $\alpha = 11$ deg at the 5b station the maximum induced rolling moment coefficient has decreased by about 10%. To explain this decrease with downstream distance we will refer to Figs. 8b and 10b. As a result of the disturbances and probable local separations of the boundary layer on the wing lower surface caused by mounting the pylons, the shear layer spiralling into the already rolled up core is interrupted. At the 5b station, for the engines mounted case, the still unrolled shear layer is further outboard of the core than for the clean wing configuration (as is clear from the bump in the total pressure loss outboard of the wingtip position in Fig. 8b). The induced tangential velocities outboard of the vortex center are consequently lower than for the clean wing configuration (see Fig. 10b). Since the trailing wing sees the whole flowfield over its 10-in. span, the reduction in the tangential velocity over a part of the flow has resulted in the observed reduction in the maximum induced rolling moment.

A comparison of the induced rolling moment coefficient with and without air injection is shown in Fig. 12, for $\alpha = 5$ and 11 deg, at both the 2½ and 5b stations. Other than small shifts in the position of the maxima (which correspond to shifts in core position), air injection at this downstream distance has only a small effect on the induced rolling moment, at least when the wing roll axis is in the vicinity of the vortex core.

Figure 13 is presented to show the lateral variation of the induced rolling moment coefficient, when the trailing wing chordal plane is at the same height as the vortex center. The maximum induced rolling moment coefficient occurs when the wing center coincides with the vortex center. The minimum induced rolling moment coefficient (the maximum negative value) occurs when the vortex center is at the trailing wingtip; the distance between the maximum and the minimum is 5 in., or half the trailing wing span.

A comparison of the measured maximum induced rolling moment coefficient and that calculated from simple strip theory using the measured flowfield (as explained in Refs. 12 and 13) is given in Table 2. Even though the calculated values are somewhat higher than those measured, because of the limitations of the theory used, the trend is the same and should give more confidence in the measured flowfield and induced rolling moment results.

Recent subscale measurements[6] behind a model of the Boeing 747, with flap deflections of the outboard and/or the inboard flap of 30 deg, show that the jet thrust has an attenuating effect on the vortex. The measured rolling moment, induced on a following model at a separation distance equivalent to 0.88 nautical miles, is reduced by approximately 20% of the zero thrust case. The results of flight tests,[7,8] using the B-747 aircraft and again with flap deflections of the outboard and/or the inboard flap of 30 deg, indicate a similar thrust attenuating effect on the vortex system. The inboard and outboard engines of the B-747 airplane are of course aligned in front of the outboard edges of the inboard and outboard flaps, respectively. With both flaps extended the dominant vortex is the vortex shed from the outboard edge of the outboard flap. With the outboard flap retracted (only the inboard extended), the dominant vortex is that shed from the outboard edge on the inboard flap. In both cases one of the engines is blowing its exhaust directly into the dominat vortex, i.e., the jet mixing region is interfering with the vortex roll-up and formation; hence the strong effect. The measurements presented in this paper only represent a cruising flight, no flaps, configuration; the dominant or only vortex is the tip vortex which is far from the jet efflux of the outboard engine and hence does not interact with the vortex formation. Also, other flight measurement made by the FAA using the C.V. 880 aircraft with a tower flyby technique[1] showed that thrust differences (namely all engines at normal power compared to two engines on one side at zero thrust) produced no noticeable changes to the vortex structures (as deduced from recorded data).

Conclusions

From these near-field experimental results, taken up to five spans (or 35$\bar{c}$) downstream of the mean 1/4 chord point of the generating wing, and with and without engine simulation, the following can be concluded:

1) For the clean wing configuration, and at the 2½ span station, it was found[13] that the shear layers, resulting from separation of the turbulent boundary layers on the main wing, had not fully rolled up and consequently the circulation around a circuit near the "core" was considerably below (only about 45%) that derived from the corresponding spanwise loading. Moving downstream to the 5 span station it was found that no further appreciable roll-up of the shear layers occurred when judged by the circulation around the core. This suggests that the shear layers are already effectively fully rolled up at the 2½ span station even though not in an axisymmetric form. There was no appreciable difference between the induced rolling moment measured on the trailing wing at the two downstream stations, consistent with the detailed flowfield measurements.

2) The mounting of two simulated engines on the main wing lower surface at representative spanwise locations, but with no exhaust jet air flow, did not greatly affect the rolled up part of the flowfield. However the pylon-nacelle systems have evidently modified the wing lower surface boundary-layer development with the result that the free shear layer in the central part of the wake (and of course the vorticity shed from that region) is highly contorted. This part of the shear layer also seems to be spiralling (rolling up) around the vortex core at a slower rate, compared to the wake configuration for the clean wing; in other words the roll-up process has been interrupted and decelerated.

3) At the 2½b downstream station the changes in the induced tangential velocity distribution and induced rolling moment coefficient on the trailing wing can be related to changes in the main wing overall lift coefficient and loading near the tip due to mounting the engines. At the 5b station there is a general decrease in the induced rolling moment coefficient, normalized to generating wing $\bar{C}_L$, of the order of 10%.

4) Air injection through the simulated engines, with $V_j/V_\infty = 1.5$, has resulted in no appreciable change in the induced rolling moment coefficient on the trailing wing, as compared to the engine mounted no-injection case. The in-

jection has resulted in small changes in the vortex core position relative to both the wingtip and to the still unrolled part of the shear layers but the core structure is essentially unchanged.

It is recognized that these conclusions are for cruising conditions and should not be generalized to far-field conditions nor to other wing configurations, for example, different engine mounting locations.

References

[1]Garodz, L. J., "Measurements of Boeing 747, Lockheed C5A and Other Aircraft Vortex Wake Characteristics by Tower Fly-by Technique," *Aircraft Wake Turbulence and its Detection*, edited by J. Olsen, A. Goldberg, and M. Rogers, Plenum Press, New York, 1971, pp. 265-286.

[2]Chigier, N. A. and Corsiglia, V. R., "Wind Tunnel Studies of Wing Wake Turbulence," *Journal of Aircraft*, Vol. 9, Dec. 1972, pp. 820-825.

[3]Wickens, R. H., "The Externally-Blown Jet Flap: A Powered-Lift Concept for STOL," *Canadian Aeronautics and Space Journal*, Vol. 20, Sept. 1974, pp. 323-340.

[4]Corsiglia, V. R., Rossow, V. J., and Ciffone, D. L., "Experimental Study of the Effects of Span Loading on Aircraft Wakes," AIAA Paper 75-885, Hartford, Connecticut, June 16-18, 1975.

[5]Ciffone, D.L., "Vortex Interaction in Multiple Vortex Wakes Behind Aircraft," *Journal of Aircraft*, Vol. 14, in press.

[6]Patterson, J. C., Jr., and Jordan, E. L., Jr., "Thrust Augmented Vortex Attenuation," *NASA Symposium on Wake Vortex Minimization*, Washington, D.C., Feb. 25-26, 1976, pp258-274.

[7]Barber, M. L., Hastings, E. C., Jr., Champine, R. A., and Tymczyszyn, J. J., "Vortex Attenuation Flight Experiments," *NASA Symposium on Wake Vortex Minimization*, Washington, D.C., Feb. 25-26, 1976.

[8]Smith, H., "Flight Test Investigation of the Rolling Moments Induced on a T-37B Airplane in the Wake of a B-747 Airplane," NASA TM X-56031, April 1975.

[9]Stickle, J. W., and Kelly, M. W., "Ground-Based Facilities for Evaluating Vortex Minimization Concepts," *NASA Symposium on Wake Vortex Minimization*, Washington, D.C., Feb. 25-26, 1976, pp. 123-154.

[10]Graham, J. A. H., Newman, B. G., and Phillips, W. R., "Turbulent Trailing Vortex with Central Jet and Wake," Paper 74-40, *Ninth Congress of the International Council of the Aeronautical Sciences*, Haifa, Israel, Aug. 1974.

[11]El-Ramly, Z., "Aircraft Trailing Vortices: A Survey of the Problem," Carleton University, Ottawa, Canada, Rept. ME/A 72-1, Nov. 1972, p. 179.

[12]El-Ramly, Z., "Investigation of the Development of the Trailing Vortex System Behind a Sweptback Wing," Carleton University, Ottawa, Canada, Rept. ME/A 75-3, Oct. 1975, p.177.

[13]El-Ramly, Z., Rainbird, W. J., and Earl D., "Some Wind Tunnel Measurements of the Trailing Vortex Development Behind a Sweptback Wing: Induced Rolling Moment on Intercepting Wings," *Journal of Aircraft*, Vol. 13, Dec. 1976, pp. 962-967.

[14]El-Ramly, Z., and Rainbird, W. J., "Computer Controlled System for the Investigation of the Flow Behind a Sweptback Wing," *Proceedings of the 9th AIAA Aerodynamic Testing Conference*, Arlington, Texas, June 7-9, 1976, pp. 119-128.

[15]DeVries, O., "Wind Tunnel Investigation of the Development of the Vortex Wake Behind a Sweptback Wing," National Aerospace Laboratory NLR, The Netherlands, TR 72017 C, March 1973.

[16]Labrujere, Th.E., and DeVries, O., "The Deformation of a Vortex Sheet Behind a Sweptback Wing, Comparison of Measurements and Calculations," *IXth ICAS Congress*, Haifa, Israel, Aug. 1974.

[17]El-Ramly, Z., "Wind Tunnel Flow Field Measurements Behind a Sweptback Wing," Lockheed Georgia Contractor Report, P.O. CK 27059P, Carleton University, Ottawa, Feb. 1976.

[18]El-Ramly, Z. and Rainbird, W. J., "Flow Survey Behind Wings," AIAA Paper 77-175, Los Angeles, Calif., Jan. 24-26, 1977.